Supporting Information

# Bio-inspired FeN$_5$ moieties anchored on three-dimensional graphene aerogel to improve oxygen reduction catalytic performance

**Jianshe Huang,[a] Qingqing Lu,[ab] Xiao Ma [ab] and Xiurong Yang*[a]**

[a] State Key Laboratory of Electroanalytical Chemistry, Changchun Institute of Applied Chemistry,

Chinese Academy of Sciences, Changchun, 130022, Jilin,China

[b] University of Chinese Academy of Sciences, Beijing, 100049, China

## 1. ORR activity measurments and related calculations

ORR activity was characterized by using cyclic volyammetry (CV) and linear sweep voltammetry (LSV) techniques. CV characterizations of the catalysts were conducted at the static state in the potential range from 0.4 V to -0.8 V with the scan rate of 50 mV s$^{-1}$.

For RDE measurements, the working electrode was scanned cathodically from 0.2 V to -0.8 V at a scan rate of 10 mV s$^{-1}$ with the rotation speed varying from 400 rpm to 2500 rpm. Koutecky-Levich plots were analyzed at various electrode potentials, and were used to calculate the number of transferred electron (n) on the basis of the Koutecky-Levich equation:

$$\frac{1}{j} = \frac{1}{j_L} + \frac{1}{j_K} = \frac{1}{B\omega^{1/2}} + \frac{1}{j_K} \tag{1}$$

$$B = 0.62nFC_0 \left(D_0\right)^{2/3} v^{-1/6} \tag{2}$$

where $j$ is the measured current density, $j_K$ is the kinetic current density, $j_L$ is the diffusion-limiting current density, $\omega$ is the angular rotation speed (rad s$^{-1}$), $F$ is Faraday constant (96485 C mol$^{-1}$), $C_0$ is the bulk concentration of $O_2$ in 0.1 M KOH solution ($1.2\times10^{-3}$ mol L$^{-1}$), $D_0$ is the diffusion coefficient of $O_2$ in 0.1 M KOH solution ($1.9\times10^{-5}$ cm$^2$ s$^{-1}$) and $v$ is the kinetic viscosity of the electrolyte (0.01 cm$^2$ s$^{-1}$).[1]

The kinetic current density was calculated from the mass-transport correction of RDE by the following equation:

$$j_K = \frac{j \times j_L}{\left(j_L - j\right)} \tag{3}$$

RRDE measurements were carried out to determine the four-electron selectivity. ORR polarization were performed by LSV from 0.2 V to -0.8 V at a scan rate of 10 mV s$^{-1}$ and 1600 rpm, and the ring potential was held at 0.3 V. The peroxide yield (%HO$_2^-$) and the number of transferred electron (n) were determined by the following equations:

$$n = \frac{4I_D}{I_D + (I_R /\!/ N)} \tag{4}$$

$$\%HO_2^- = 100\frac{2I_R / N}{I_D + (I_R / N)} \tag{5}$$

Where $I_D$ represents the disk current, $I_R$ represents the ring current, and $N$ is the RRDE collection coefficient at the ring (0.37).

For commercial Pt/C catalyst, ORR polarization plot was scanned anodically from -0.8 V to 0.2 V at the scan rate of 10 mV s$^{-1}$ due to the irreversible nature of the Pt surface hydroxide/oxide formation.[2] All the ORR polarization current density presented in the figures were corrected by subtracting the background current obtained in N$_2$-saturated electrolyte, and have been normalized to the electrode geometric surface area. Onset potential (E$_{onset}$) is defined as the potential that is able to generate a current density of 0.1 mA cm$^{-2}$ during the ORR based on the recorded steady state polarization curves, and the potential corresponding to 50% of the diffusion-limiting current density was defined as the half-wave potential (E$_{1/2}$).
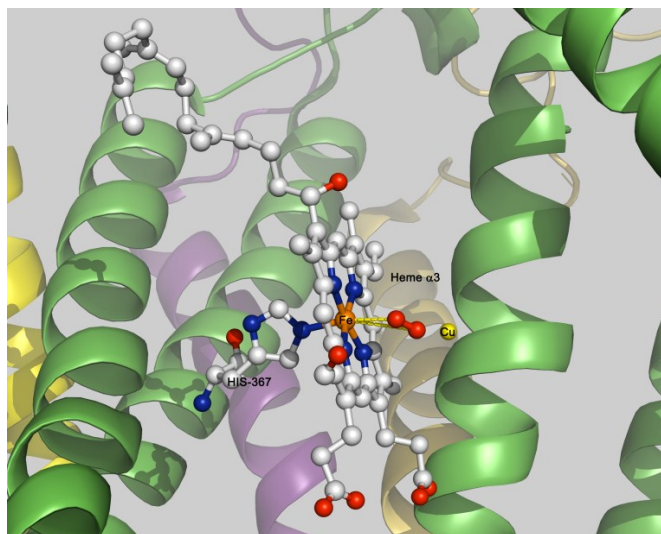
## 2. Supporting figures



**Figure S1.** Crystal structure of the Heme $\alpha_3$ active site with $O_2$ bonding in Cytochrome c oxidase (CcO) from bovine heart (PDB ID code 2Y69).[3] The central iron atom in Heme $\alpha 3$ site forms five-coordinated structure ($FeN_5$) with an axial histidine ligand.
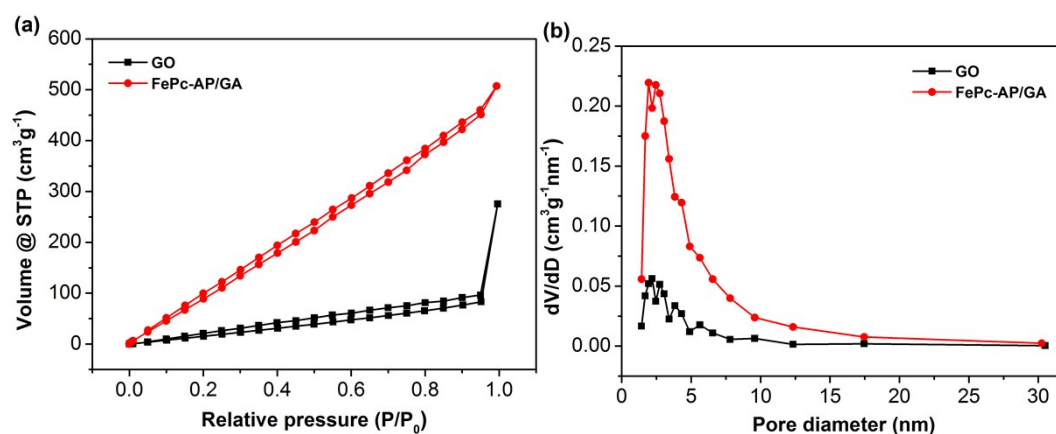


**Figure S2.** (a) Nitrogen adsorption and desorption isotherms and (b) BJH pore size distribution of freeze-dried FePc/AP-GA and GO.
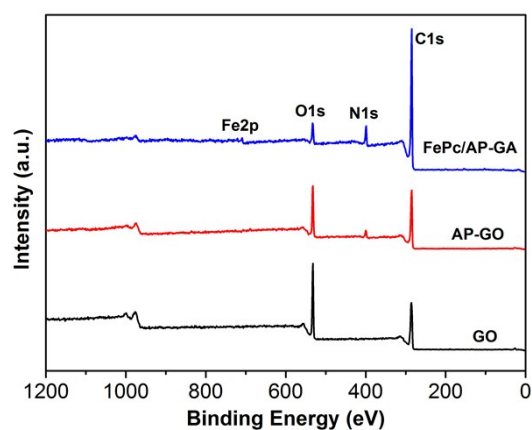
**Figure S3.** XPS survey spectra of GO, AP-GO, and FePc/AP-GA.

**Table S1.** Elemental quantification of GO, AP-GO and FePc/AP-GO determined by using XPS.

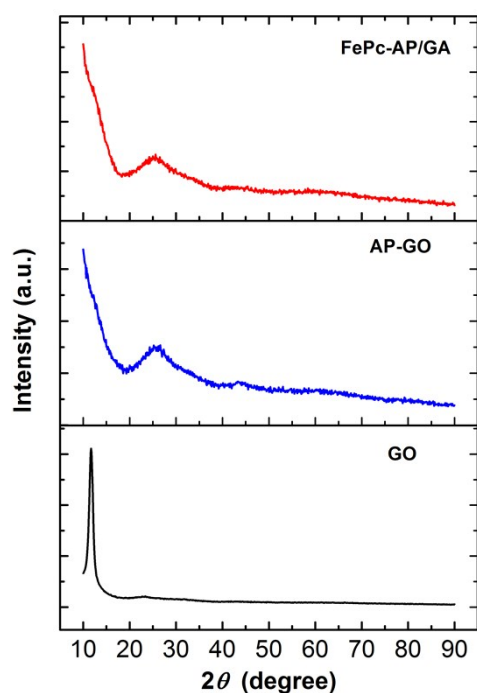| Sample | C (at%) | O (at%) | N(at%) | Fe (at%) |
|---|---|---|---|---|
| GO | 72.42 | 27.58 | -- | -- |
| AP-GO | 72.38 | 23.01 | 4.61 | -- |
| FePc/AP-GA | 85.09 | 3.98 | 10.23 | 0.69 |

**Figure S4.** XRD patterns of GO, AP-GO, and FePc/AP-GA.

XRD analysis was performed to investigate the exfoliation of GO and the functionalized graphene sheets. As shown in Figure S4, GO exhibits a sharp peak at 11.7° with a d-spacing of 7.57 Å, which is consistent with the previously reported results.[4] This value is much larger than that of natural graphite (3.36 Å),[5] suggesting a large number of oxygenated functional groups were introduced into the interlayer space of graphite flake. For AP-GO and FePc/AP-GA, the main diffraction peak appeared at about 25°, which was ascribed to (002) plane of carbon material. The calculated interlayer spacing were 3.53 and 3.45 Å for AP-GO and FePc/AP-GA, respectively, which are much lower than GO precursor, while slightly larger than natural graphite. These results suggested the existence of π-π stacking between graphene sheets after the functionalization. Simultaneously, the residual oxygenated functional groups and the immobilized FePc molecules impeded the reduced GO (rGO) sheets to irreversibly agglomerate or restack. The broad diffraction peak of

6

FePc/AP-GA implied the poor ordering of graphene sheets stacking and reflected the FePc/AP-GA framework is composed of few-layer stacked graphene sheets.

**Table S2.** Comparison of the ORR activity of the synthesized catalysts with the benchmarked Pt/C catalyst.

| Sample | CV $E_p$ (V) | CV $i_p$ (mA) | LSV $E_{onset}$ (V) | LSV $E_{1/2}$ (V) | j @-0.4 V (mA cm$^{-2}$) |
|---|---|---|---|---|---|
| GA | -0.275 | 0.151 | -0.084 | -0.233 | 2.049 |
| AP-GA | -0.231 | 0.253 | -0.037 | -0.181 | 2.764 |
| FePc+AP-GA | -0.078 | 0.306 | 0.046 | -0.075 | 5.341 |
| FePc/AP-GA | -0.040 | 0.511 | 0.066 | -0.035 | 5.983 |
| Pt/C | -0.083 | 0.425 | 0.100 | -0.057 | 5.503 |

**Table S3.** Comparison of the ORR activity between FePc/AP-GA and other non-pyrolyzed NPMCs under alkaline condition in literature. Test conditions: electrolyte, 0.1 M KOH; rotating speed, 1600 rpm.

| Catalyst | Loading (mg cm$^{-2}$) | $E_{onset}$ (V vs. RHE) | $E_{1/2}$ (V vs. RHE) | $j_k$ or $j_L$ (mA cm$^{-2}$) | Ref. |
|---|---|---|---|---|---|
| FePc/AP-GA | 0.404 | 0.973 | 0.872 | $j_L$=5.98@0.507V $j_k$=20.01@0.807V | This work |
| Fe-SPc/KJ300 | 0.612 | | 0.611 | | [6] |
| FePc-Py-CNTs | 0.318 | | 0.915 | | [7] |
| [CoN$_4$]$_3$/C | 0.0255 | 0.837 | | $j_k$=9.63 @0.35V | [8] |
| [FeN$_4$]$_3$/C | | 0.827 | | $j_k$=4.80 @0.35V | |
| (G-dye 50 wt %-FeP)$_n$ MOF | 0.159 | 0.93 | | $j_k$=5.88 @-0.65V | [9] |
| FePc/NG | 0.051 | 0.956 | | | [10] |
| FePc/rGO | | 0.936 | | | |
| Graphene-FePc | 0.041 | 0.98 | 0.88 | | [11] |
| FePc-Gr | 0.423 | 0.99 | | | [12] |
| CoTNPc/PGr | 0.17 | 0.908 | | | [13] |

| | | | | | |
|---|---|---|---|---|---|
| rGO/(Co$^{2+}$-THPP)$_7$ | 0.035 | | | $j_L$=4.0 @0.04V | [14] |
| FePc/rGO | 0.1 | 0.958 | | | [15] |
| FePc/OMC | | 0.950 | 0.892 | $j_L$=2.875 | [16] |
| FePc/MCV | 0.214 | 0.940 | 0.863 | $j_L$=2.103 | |
| FePc/RGO | | 0.893 | 0.834 | $j_L$=1.714 @0.4V, 900rpm | |
| FePPc/PSS-Gr | 0.283 | 0.928 | 0.818 | $j_L$=5.90 @0.208V | [17] |
| (DFTPP)Fe-Im-CNTs | 1.0 | | 0.922 | | [18] |
| FeTPPc/Gr | 0.21 | 0.988 | 0.895 | $j_L$=5.798 | [19] |
| Co$^{II}$-A-rG-O | 0.6 | 0.88 | 0.81 | $j_k$=8.9 @0.8V | [20] |
| rGO-TADPyCu | 0.6 | 0.951 | 0.795 | | [21] |
| Nano-CuS@Cu-BTC | 0.212 | 0.91 | | | [22] |
| Ni$_3$(HITP)$_2$ MOF | | 0.82 | | | [23] |
| rGO/(Ni$^{2+}$/THPP/Co$^{2+}$/THPP)$_8$ | | 0.84 | | $j_L$=3.3 @0.1V | [24] |
| MWCNT-CoTPP | | 0.78 | | | [25] |
| MWCNT-CoTCPP | | 0.82 | | | |
| MWCNT-CoTHPP | | 0.81 | | | |
| PVI-Cu(phen$^{NO_2}$)-PVI@CNTs | 1.0 | 1.046 | 0.859 | | [26] |
| shaking FePc/MWNTs | 0.3 | 0.971 | 0.864 | | [27] |
| sonicating FePc/MWNTs | | 0.959 | 0.844 | | |
| refluxing FePc/MWNTs | | 0.956 | 0.835 | | |
| Pc-FePc/Mn-GCB | 0.1 | | 0.90 | $j$=2.25 @0.9V | [28] |
| FePc-R25 | | 1.0 | 0.92 | | [29] |
| Cu$_3$(7-N-Etppz(CH$_2$OH)) CB/SPCE | | 0.92 | 0.81 | | [30] |

Potential conversion of Ag/AgCl electrode, SCE, and Hg/HgO electrode into RHE scale were achieved according to Nernst equation: $E$(RHE) = $E$(Reference electrode *versus* NHE) + (0.059 V)×(pH). The value of $E$(Reference electrode *versus* NHE) was adopted from the book written by Hamann et al.[31]

$E$(RHE)= $E$(Ag/AgCl, sat. KCl) + 0.199 + 0.059pH.

$E$ (RHE) =$E$ (Ag/AgCl, 3.5 M KCl) + 0.205 + 0.059pH.

$E$ (RHE) =$E$ (Ag/AgCl, 3 M KCl) + 0.210 + 0.059pH.

$E$(RHE)= $E$(SCE, sat. KCl) + 0.241 + 0.059pH.

$E$ (RHE) = $E$ (Hg/HgO, 1 M NaOH) + 0.140 V + 0.059pH.

**Table S4.** Comparison of the ORR activity between FePc/AP-GA and other pyrolyzed graphene-based NPMCs under alkaline condition in literature. Test conditions: electrolyte, 0.1 M KOH; rotating speed, 1600 rpm.

| Catalyst | Loading (mg cm$^{-2}$) | $E_{onset}$ (V vs. RHE) | $E_{1/2}$ (V vs. RHE) | $j_k$ or $j_L$ (mA cm$^{-2}$) | Ref. |
|---|---|---|---|---|---|
| FePc/AP-GA | 0.404 | 0.973 | 0.872 | $j_L$=5.98@0.507V $j_k$=20.01@0.807V | This work |
| Co$_3$O$_4$/rmGO | 0.17 | 0.88 | 0.79 | | [32] |
| Co$_3$O$_4$/N-rmGO | | | 0.83 | | |
| GN-ZnSe | 0.063 | 0.827 | | | [33] |
| Co$_{1-x}$S/RGO | 0.1 | 0.87 | | $j_L$=5.8 @0.3V | [34] |
| G-Co/CoO | | 0.796 | | | [35] |
| MnCo$_2$O$_4$/N-rmGO | 0.1 | 0.93 | | | [36] |
| FeNGr3 | | 0.917 | | | [37] |
| NG/Fe$_{5.0}$ | 0.051 | 0.937 | | $j_k$=8.20 @0.577V | [38] |
| Fe$_3$O$_4$/N-GAs | | 0.787 | | | [39] |
| Mn$_3$O$_4$-NG | 0.2 | 0.887 | | $j$=3.7 @0.577V | [40] |
| Fe-NG-30 | 0.4 | 0.985 | 0.898 | $j_k$=0.23 @0.978V | [41] |
| TiN/NG | 0.2 | 0.836 | | | [42] |
| N-rGO-Mn$_3$O$_4$ | 0.1 | 0.933 | | | [43] |
| Mn$_3$O$_4$-NG | 0.1 | 0.847 | | $j_k$=11.69 @0.377V | [44] |
| Fe-N-graphene | 0.4 | 1.01 | | | [45] |
| N-doped Fe/Fe$_3$C@C/RGO | 0.708 | 1.0 | 0.93 | $j_k$=30.25 @0.7 V | [46] |
| N-Fe-MOF | 1.0 | | 0.88 | | [47] |
| N-CG-CoO | 0.707 | 0.90 | | | [48] |
| Fe$_x$N/NGA | 0.051 | 0.966 | | | [49] |
| Fe$_3$C-GNRs | | 0.95 | 0.78 | $j_k$=4.8 @0.5V | [50] |
| N/Co-doped PCP//NRGO | 0.714 | 0.97 | | $j_L$=7.53 @0.4V | [51] |
| N-Fe-G | 0.05 | 0.892 | | $j_L$=5.28 @0.4V | [52] |
| Co-CoO/N-rGO | 0.21 | 0.88 | 0.78 | | [53] |
| CoFe$_2$O$_4$/NG | 0.283 | 0.947 | 0.833 | | [54] |
| GPFe | | 0.916 | | $j_L$=6.72 @0.166V | [55] |
| Co$_3$O$_4$-PPy/GN | 0.2 | 0.848 | 0.77 | $j_L$=4.471 | [56] |
| ZIF/rGO-700-AL | 0.408 | 0.93 | | $j_L$=5.49 @0.7V | [57] |
| Co-N/RGO | 0.383 | 0.876 | 0.796 | $j_L$=4.47 | [58] |
| Co-N/HGS | | 1.006 | 0.896 | $j_L$=6.30 | |
| Fe3-NG | 0.5 | 0.965 | 0.826 | $j_L$=7.20 @0.4V | [59] |
| N-Co$_9$S$_8$/G | 0.2 | 0.941 | | | [60] |
| PANI-Fe-rGO | | 1.05 | 0.89 | $j_L$=3.8 | [61] |
| Me-Fe-rGO | 0.6 | 1.05 | 0.87 | $j_L$=3.3 | |
| EDA-Fe-rGO | | 0.94 | 0.80 | $j_L$=3.2 | |

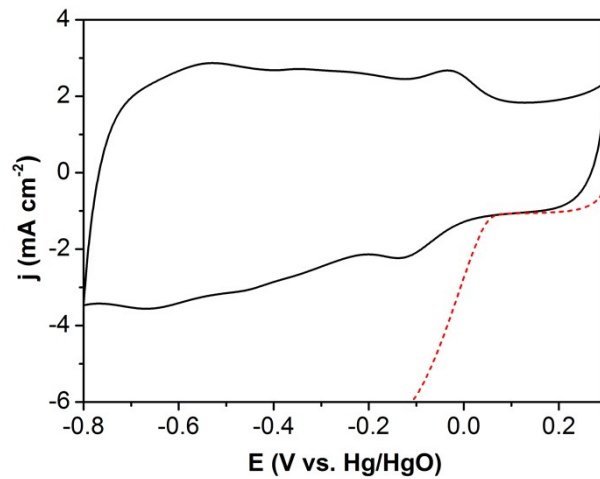| | | | | | |
|---|---|---|---|---|---|
| CoS/NSGA | | 0.971 | 0.797 | $j_L$=5.1 @0.2V | [62] |
| EA-SFeNG | 0.5 | 1.02 | 0.848 | | [63] |
| FeNpGr | 0.707 | 0.90 | | | [64] |
| Fe/Co-NpGr | | 0.93 | | | |
| Fe-N/R3DG | 0.15 | 0.98 | 0.82 | $j_L$=6.5@0.4V | [65] |
| Co-N-GA | 0.281 | 0.9 | | $j_L$=6.0 | [66] |
| Fe$_2$P/NPFG | 0.269 | 0.97 | 0.83 | $j_L$=5.02 | [67] |
| Fe$_2$N/NSG | | 0.97 | 0.82 | $j_L$=5.21 | |
| Ni$_3$FeN/NRGO | 0.1 | 0.9 | | | [68] |
| Fe-N-CIG | 0.23 | | 0.84 | | [69] |
| Co-S/SNGA | 0.286 | 1.0 | | $j_L$=4.6 | [70] |
| AgNW-GA | 0.204 | 0.905 | | $j_L$=3.72 | [71] |
| CoMn/pNGr | | 0.94 | 0.791 | | [72] |
| LaNiO$_3$/N,S-Gr | 0.349 | 0.927 | 0.797 | | [73] |
| CoO$_x$ NPs/BNG | | 0.95 | 0.805 | $j_L$=5.67 @0.2V | [74] |
| NS/rGO-Co | 0.485 | 0.97 | 0.84 | $j_L$=5.964 | [75] |
| GO/ZIF-8@ZIF-67-900 | 0.1 | 0.93 | | $j_k$=10.0 @0.8V | [76] |
| CoO$_x$/NG-A | 0.1 | 1.019 | | $j_k$=32.5 @0.75V | [77] |
| DG@FeCo | 0.16 | 0.92 | 0.815 | | [78] |
| Ni-MnO/rGO aerogels | 0.25 | 0.94 | 0.78 | | [79] |
| GL-Fe/Fe$_5$C$_2$/NG-800 | 0.15 | 0.98 | 0.86 | | [80] |
| S-Co$_{9-x}$Fe$_x$S$_8$@rGO | 0.5 | 0.94 | 0.84 | | [81] |
| Fe$_{0.5}$Ni$_{0.5}$@N-GR | 0.2 | 0.94 | 0.83 | $j_L$=4.05 @0.2V | [82] |
| mNC-Fe$_3$O$_4$@rGO | 0.24 | 0.95 | 0.84 | $j_L$=5.7 @0.4V | [83] |



**Figure S5.** Cyclic voltammogram (black solid line) and ORR polarization curve (red dash line) collected for FePc/AP-GA in O$_2$-saturated 0.1 M KOH electrolyte. Scan rate, CV: 20 mV s$^{-1}$, LSV: 10 mV s$^{-1}$ with a rotation rate of 1600 rpm.
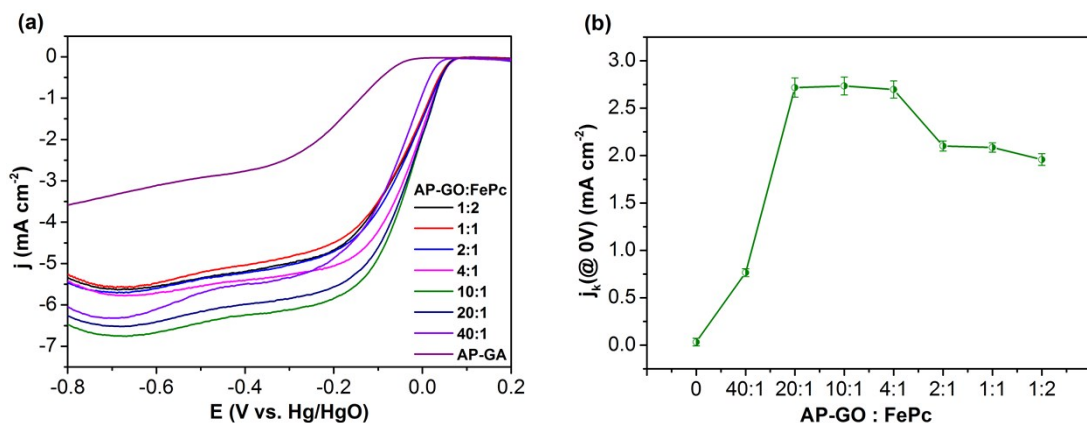
**Figure S6.** The effect of ratio of AP-GO to FePc (m : m) on the catalytic activity of the as-prepared catalysts. (a) ORR polarization curves of catalysts in $O_2$-saturated 0.1 M KOH electrolyte. (b) Plots of diffusion-corrected current density at 0 V versus AP-GO : FePc (m : m).
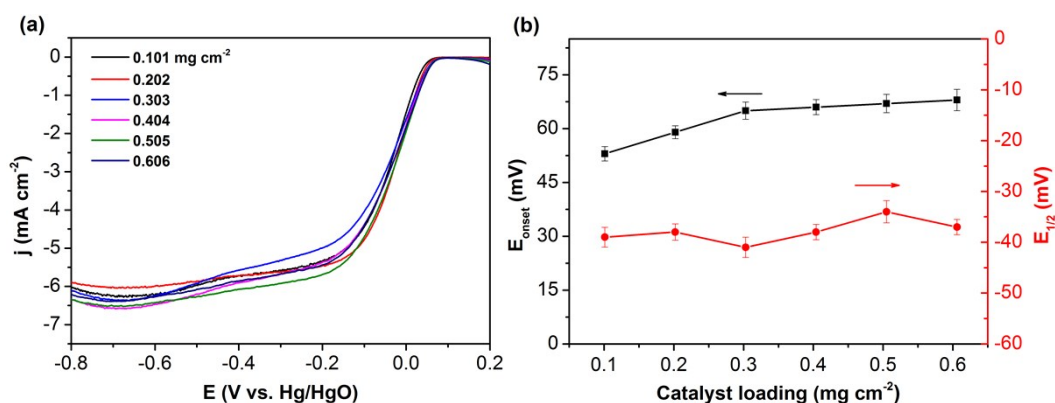


**Figure S7.** The effect of catalyst loading on the ORR responses of FePc/AP-GA catalyst. (a) ORR polarization curves of the electrodes with different catalyst loading in $O_2$-saturated 0.1 M KOH electrolyte. (b) Plots of $E_{onset}$ (black line) and $E_{1/2}$ (red line) versus catalyst loading.

**Figure S8.** Rotating-disk voltammograms in $O_2$-saturated 0.1 M KOH at a scan rate of 10 mV s$^{-1}$ and different rotating speeds, and the corresponding Koutecky–Levich plots at different potentials. (a, b) Pt/C, (c, d) FePc+AP-GA, and (e, f) FePc/AP-GA.
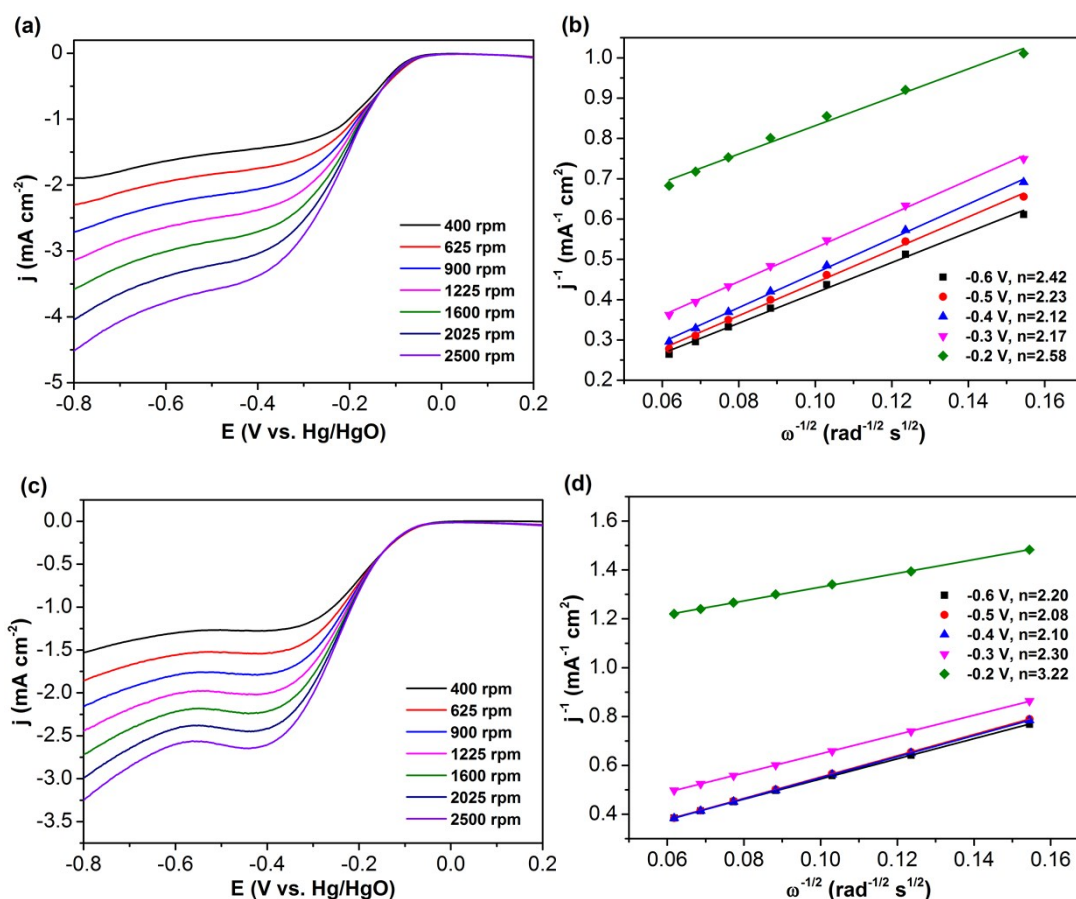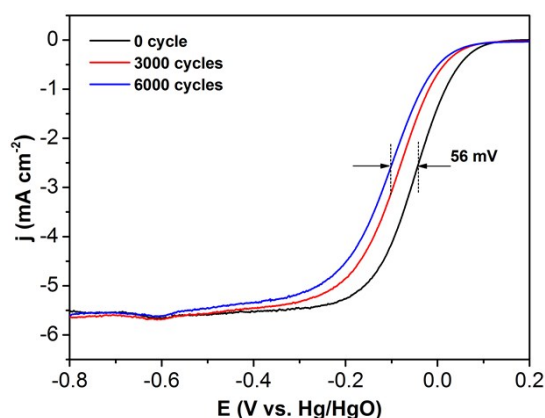
**Figure S9.** Rotating-disk voltammograms in O$_2$-saturated 0.1 M KOH at a scan rate of 10 mV s$^{-1}$ and different rotating speeds, and the corresponding Koutecky–Levich plots at different potentials. (a, b) AP-GA, and (c, d) GA.



**Figure S10.** Accelerated stability test (AST) of Pt/C catalyst by continuous potential cycling in O$_2$-saturated 0.1 M KOH solution between -0.35 V and 0.15 V. LSV scan rate, 10 mV s$^{-1}$; rotation rate, 1600 rpm.

After 6000 potential cycles, the $E_{1/2}$ was negatively shifted by 56 mV due to the dissolution/ agglomeration of Pt nanoparticles.
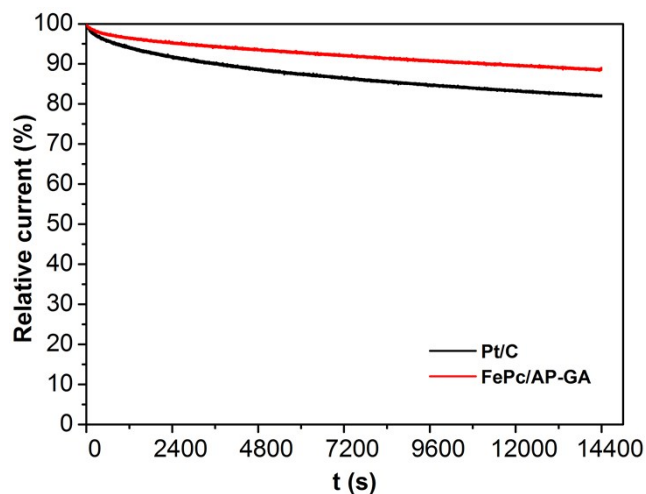


**Figure S11.** Chronoamperometric responses (percentage of current retained versus operation time) of FePc/AP-GA and Pt/C catalyst at -0.20 V in $O_2$-aturated 0.1 M KOH electrolyte. Rotation rate, 900 rpm.
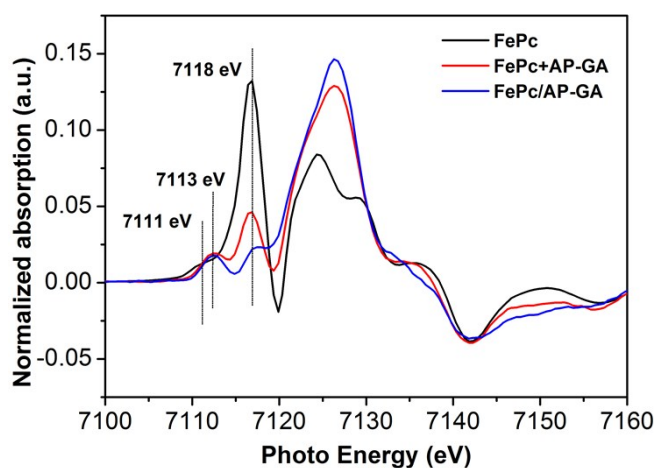


**Figure S12.** First derivative spectra of the Fe K-edge XANES of FePc, FePc+AP-GA, and FePc/AP-GA samples.
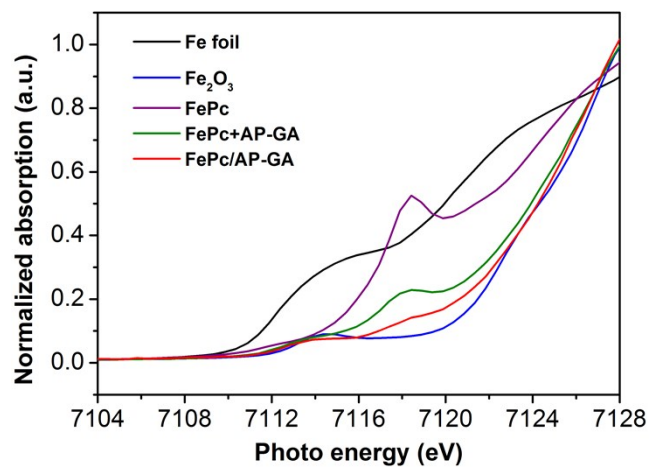
**Figure S13.** A zoomed-in view of the pre-edge region of Fe K-edge XANES .
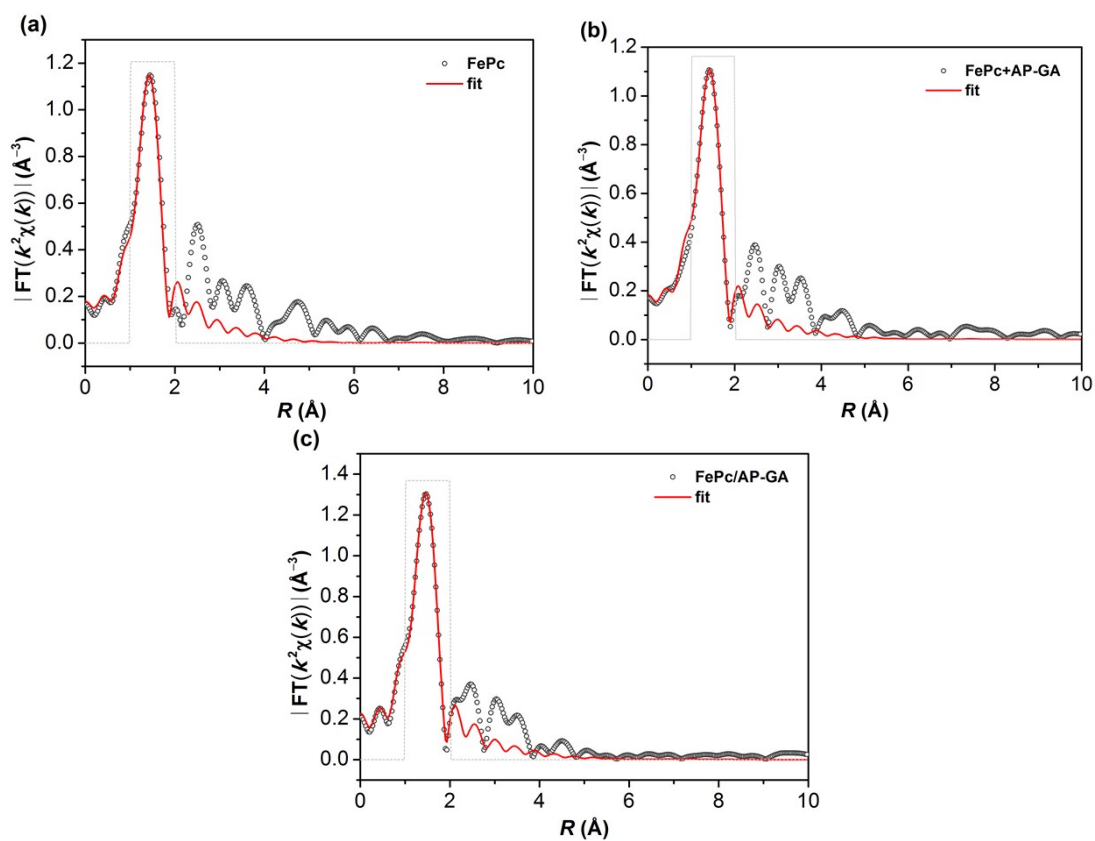


**Figure S14.** FT-EXAFS and the corresponding fitting curves of (a) FePc, (b) FePc+AP-GA, and (c) FePc/AP-GA. Measured and calculated spectra are well matched for all samples. The best-fit parameters are shown in Supplementary Table S5.

**Table S5.** Fe K-edge EXAFS fitting parameters for various samples.

| Sample | shell | $N^a$ | $R$ (Å)$^b$ | $\sigma^2$ (×10$^{-3}$ Å$^2$)$^c$ | $\Delta E_0$ (eV)$^d$ | R factor (%)$^e$ |
|---|---|---|---|---|---|---|
| FePc | Fe-N | 4 | 1.93 | 3.0 | 2.62 | 0.18 |
| FePc/GA | Fe-N | 4.2 | 1.98 | 4.2 | -3.89 | 0.10 |
| FePc-AP/GA | Fe-N | 4.7 | 2.01 | 3.6 | -2.21 | 0.12 |

$^a N$: coordination numbers; $^b R$: bond distance; $^c \sigma^2$: Debye-Waller factors; $^d \Delta E_0$: the inner potential correction; $^e R$ factor: goodness of fit. $S_0^2 = 0.80$ was fixed to all the samples. Error bounds (accuracies) that characterize the structural parameters obtained by EXAFS spectroscopy were estimated as $N \pm 20\%$; $R \pm 1\%$; $\sigma^2 \pm 20\%$; $\Delta E_0 \pm 20\%$.

**References**

1. M. Xiao, J. Zhu, L. Feng, C. Liu and W. Xing, *Adv. Mater.*, 2015, **27**, 2521.
2. H. T. Chung, J. H. Won and P. Zelenay, *Nat. Commun.*, 2013, **4**, 1922.
3. V. R. I. Kaila, E. Oksanen, A. Goldman, D. A. Bloch, M. I. Verkhovsky, D. Sundholm and M. Wikström, *Biochim. Biophys. Acta*, 2011, **1807**, 769.
4. H. Yang, C. Shan, F. Li, D. Han, Q. Zhang and L. Niu, *Chem. Commun.*, 2009, **26**, 3880.
5. Y. Xu, K. Sheng, C. Li and G. Shi, *ACS Nano*, 2010, **4**, 4324.
6. W. Li, A. Yu, D. C. Higgins, B. G. Llanos and Z. Chen, *J. Am. Chem. Soc.*, 2010, **132**, 17056.
7. R. Cao, R. Thapa, H. Kim, X. Xu, M. Gyu Kim, Q. Li, N. Park, M. Liu and J. Cho, *Nat. Commun.*, 2013, **4**, 2076.
8. R. Liu, C. von Malotki, L. Arnold, N. Koshino, H. Higashimura, M. Baumgarten and K. Müllen, *J. Am. Chem. Soc.*, 2011, **133**, 10372.
9. M. Jahan, Q. Bao and K. P. Loh, *J. Am. Chem. Soc.*, 2012, **134**, 6707.
10. C. Zhang, R. Hao, H. Yin, F. Liu and Y. Hou, *Nanoscale*, 2012, **4**, 7326.
11. Y. Jiang, Y. Lu, X. Lv, D. Han, Q. Zhang, L. Niu and W. Chen, *ACS Catal.*, 2013, **3**, 1263.
12. Y. Liu, Y.-Y. Wu, G.-J. Lv, T. Pu, X.-Q. He and L.-L. Cui, *Electrochim. Acta*, 2013, **112**, 269.
13. G. Lv, L. Cui, Y. Wu, Y. Liu, T. Pu and X. He, *Phys. Chem. Chem. Phys.*,

2013, **15**, 13093.

14. H. Tang, H. Yin, J. Wang, N. Yang, D. Wang and Z. Tang, *Angew. Chem. Int. Ed.*, 2013, **52**, 5585.

15. I. Kruusenberg, J. Mondal, L. Matisen, V. Sammelselg and K. Tammeveski, *Electrochem. Commun.*, 2013, **33**, 18.

16. M. Li, X. Bo, Y. Zhang, C. Han and L. Guo, *J. Power Sources*, 2014, **264**, 114.

17. L. Lin, M. Li, L. Jiang, Y. Li, D. Liu, X. He and L. Cui, *J. Power Sources*, 2014, **268**, 269.

18. P.-J. Wei, G.-Q. Yu, Y. Naruta and J.-G. Liu, *Angew. Chem. Int. Ed.*, 2014, **53**, 6659.

19. L. Cui, G. Lv and X. He, *J. Power Sources*, 2015, **282**, 9.

20. J. Han, Y. J. Sa, Y. Shim, M. Choi, N. Park, S. H. Joo and S. Park, *Angew. Chem. Int. Ed.*, 2015, **54**, 12622.

21. Y.-T. Xi, P.-J. Wei, R.-C. Wang and J.-G. Liu, *Chem. Commun.*, 2015, **51**, 7455.

22. K. Cho, S.-H. Han and M. P. Suh, *Angew. Chem. Int. Ed.*, 2016, **55**, 15301.

23. E. M. Miner, T. Fukushima, D. Sheberla, L. Sun, Y. Surendranath and M. Dincă, *Nat. Commun.*, 2016, **7**, 10942.

24. J. Sun, H. Yin, P. Liu, Y. Wang, X. Yao, Z. Tang and H. Zhao, *Chem. Sci.*, 2016, **7**, 5640.

25. P. K. Sonkar, K. Prakash, M. Yadav, V. Ganesan, M. Sankar, R. Gupta and D. K. Yadav, *J. Mater. Chem. A*, 2017, **5**, 6263.

26. F.-F. Wang, Y.-M. Zhao, P.-J. Wei, Q.-L. Zhang and J.-G. Liu, *Chem. Commun.*, 2017, **53**, 1514.

27. J. Yang, F. Toshimitsu, Z. Yang, T. Fujigaya and N. Nakashima, *J. Mater. Chem. A*, 2017, **5**, 1184.

28. Z. Zhang, M. Dou, J. Ji and F. Wang, *Nano Energy*, 2017, **34**, 338.

29. J. Guo, X. Yan, Q. Liu, Q. Li, X. Xu, L. Kang, Z. Cao, G. Chai, J. Chen, Y. Wang and J. Yao, *Nano Energy*, 2018, **46**, 347.

30. N. Thiyagarajan, D. Janmanchi, Y. F. Tsai, W. H. Wanna, R. Ramu, S. I. Chan, J. M. Zen and S. S. F. Yu, *Angew. Chem. Int. Ed.*, 2018, **57**, 3612.

31. C. H. Hamann, A. Hamnett and W. Vielstich, *Electrochemistry*, Weinhein: Wiley-VCH, 1998.

32. Y. Liang, Y. Li, H. Wang, J. Zhou, J. Wang, T. Regier and H. Dai, *Nat. Mater.*, 2011, **10**, 780.

33. P. Chen, T.-Y. Xiao, H.-H. Li, J.-J. Yang, Z. Wang, H.-B. Yao and S.-H. Yu, *ACS Nano*, 2012, **6**, 712.

34. H. Wang, Y. Liang, Y. Li and H. Dai, *Angew. Chem. Int. Ed.*, 2011, **50**, 10969.

35. S. Guo, S. Zhang, L. Wu and S. Sun, *Angew. Chem. Int. Ed.*, 2012, **51**, 11770.

36. Y. Liang, H. Wang, J. Zhou, Y. Li, J. Wang, T. Regier and H. Dai, *J. Am. Chem. Soc.*, 2012, **134**, 3517.

37. T. Palaniselvam, H. B. Aiyappa and S. Kurungot, *J. Mater. Chem.*, 2012, **22**, 23799.

38. K. Parvez, S. Yang, Y. Hernandez, A. Winter, A. Turchanin, X. Feng and K.

Müllen, *ACS Nano*, 2012, **6**, 9541.

39. Z.-S. Wu, S. Yang, Y. Sun, K. Parvez, X. Feng and K. Müllen, *J. Am. Chem. Soc.*, 2012, **134**, 9082.

40. J. Duan, Y. Zheng, S. Chen, Y. Tang, M. Jaroniec and S. Qiao, *Chem. Commun.*, 2013, **49**, 7705.

41. B. J. Kim, D. U. Lee, J. Wu, D. Higgins, A. Yu and Z. Chen, *J. Phys. Chem. C*, 2013, **117**, 26501.

42. M. Liu, Y. Dong, Y. Wu, H. Feng and J. Li, *Chem. Eur. J.*, 2013, **19**, 14781.

43. S. Bag, K. Roy, C. S. Gopinath and C. R. Raj, *ACS Appl. Mater. Interfaces*, 2014, **6**, 2692.

44. J. Duan, S. Chen, S. Dai and S. Z. Qiao, *Adv. Funct. Mater.*, 2014, **24**, 2072.

45. C. He, J. J. Zhang and P. K. Shen, *J. Mater. Chem. A*, 2014, **2**, 3231.

46. Y. Hou, T. Huang, Z. Wen, S. Mao, S. Cui and J. Chen, *Adv. Energy Mater.*, 2014, **4**, 1400337.

47. Q. Li, P. Xu, W. Gao, S. Ma, G. Zhang, R. Cao, J. Cho, H.-L. Wang and G. Wu, *Adv. Mater.*, 2014, **26**, 1378.

48. S. Mao, Z. Wen, T. Huang, Y. Hou and J. Chen, *Energy Environ. Sci.*, 2014, **7**, 609.

49. H. Yin, C. Zhang, F. Liu and Y. Hou, *Adv. Funct. Mater.*, 2014, **24**, 2930.

50. X. Fan, Z. Peng, R. Ye, H. Zhou and X. Guo, *ACS Nano*, 2015, **9**, 7407.

51. Y. Hou, Z. Wen, S. Cui, S. Ci, S. Mao and J. Chen, *Adv. Funct. Mater.*, 2015, **25**, 872.

52. Q. Lai, Q. Gao, Q. Su, Y. Liang, Y. Wang and Z. Yang, *Nanoscale*, 2015, **7**, 14707.

53. X. Liu, W. Liu, M. Ko, M. Park, M. G. Kim, P. Oh, S. Chae, S. Park, A. Casimir, G. Wu and J. Cho, *Adv. Funct. Mater.*, 2015, **25**, 5799.

54. L. Lu, Q. Hao, W. Lei, X. Xia, P. Liu, D. Sun, X. Wang and X. Yang, *Small*, 2015, **11**, 5833.

55. F. Razmjooei, K. P. Singh, E. J. Bae and J.-S. Yu, *J. Mater. Chem. A*, 2015, **3**, 11031.

56. G. Ren, Y. Li, Z. Guo, G. Xiao, Y. Zhu, L. Dai and L. Jiang, *Nano Research*, 2015, **8**, 3461.

57. J. Wei, Y. Hu, Z. Wu, Y. Liang, S. Leong, B. Kong, X. Zhang, D. Zhao, G. P. Simon and H. Wang, *J. Mater. Chem. A*, 2015, **3**, 16867.

58. Q. Yu, J. Xu, C. Wan, C. Wu and L. Guan, *J. Mater. Chem. A*, 2015, **3**, 16419.

59. X. Cui, S. Yang, X. Yan, J. Leng, S. Shuang, P. M. Ajayan and Z. Zhang, *Adv. Funct. Mater.*, 2016, **26**, 5708.

60. S. Dou, L. Tao, J. Huo, S. Wang and L. Dai, *Energy Environ. Sci.*, 2016, **9**, 1320.

61. W. Gao, D. Havas, S. Gupta, Q. Pan, N. He, H. Zhang, H.-L. Wang and G. Wu, *Carbon*, 2016, **102**, 346.

62. Z. Luo, C. Tan, X. Zhang, J. Chen, X. Cao, B. Li, Y. Zong, L. Huang, X. Huang, L. Wang, W. Huang and H. Zhang, *Small*, 2016, **12**, 5920.

63. S. Oh, J. Kim, M. Kim, D. Nam, J. Park, E. Cho and H. Kwon, *J. Mater.*

*Chem. A*, 2016, **4**, 14400.

64. T. Palaniselvam, V. Kashyap, S. N. Bhange, J.-B. Baek and S. Kurungot, *Adv. Funct. Mater.*, 2016, **26**, 2150.

65. Y. Qin, J. Yuan, L. Zhang, B. Zhao, Y. Liu, Y. Kong, J. Cao, F. Chu, Y. Tao and M. Liu, *Small*, 2016, **12**, 2549.

66. Z. Zhu, Y. Yang, Y. Guan, J. Xue and L. Cui, *J. Mater. Chem. A*, 2016, **4**, 15536.

67. Y.-R. Chen, Q. Wang, X. Bai, Z. Yan, Y. Ning, F. He, Z. Wu and J. Zhang, *Dalton Trans.*, 2017, **46**, 16885.

68. Y. Fan, S. Ida, A. Staykov, T. Akbay, H. Hagiwara, J. Matsuda, K. Kaneko and T. Ishihara, *Small*, 2017, **13**, 1700099.

69. D. He, Y. Xiong, J. Yang, X. Chen, Z. Deng, M. Pan, Y. Li and S. Mu, *J. Mater. Chem. A*, 2017, **5**, 1930.

70. G. He, M. Qiao, W. Li, Y. Lu, T. Zhao, R. Zou, B. Li, J. A. Darr, J. Hu, M.-M. Titirici and I. P. Parkin, *Adv. Sci.*, 2017, **4**, 1600214.

71. S. Hu, T. Han, C. Lin, W. Xiang, Y. Zhao, P. Gao, F. Du, X. Li and Y. Sun, *Adv. Funct. Mater.*, 2017, **27**, 1700041.

72. S. K. Singh, V. Kashyap, N. Manna, S. N. Bhange, R. Soni, R. Boukherroub, S. Szunerits and S. Kurungot, *ACS Catal.*, 2017, **7**, 6700.

73. T. D. Thanh, N. D. Chuong, J. Balamurugan, H. Van Hien, N. H. Kim and J. H. Lee, *Small*, 2017, **13**, 1701884.

74. Y. Tong, P. Chen, T. Zhou, K. Xu, W. Chu, C. Wu and Y. Xie, *Angew. Chem. Int. Ed.*, 2017, **56**, 7121.

75. N. Wang, L. Li, D. Zhao, X. Kang, Z. Tang and S. Chen, *Small*, 2017, **13**, 1701025.

76. J. Wei, Y. Hu, Y. Liang, B. Kong, Z. Zheng, J. Zhang, S. P. Jiang, Y. Zhao and H. Wang, *J. Mater. Chem. A*, 2017, **5**, 10182.

77. W. Xia, C. Qu, Z. Liang, B. Zhao, S. Dai, B. Qiu, Y. Jiao, Q. Zhang, X. Huang, W. Guo, D. Dang, R. Zou, D. Xia, Q. Xu and M. Liu, *Nano Lett.*, 2017, **17**, 2788.

78. X. Yan, Y. Jia, L. Zhang, M. Teng Soo and X. Yao, *Chem. Commun.*, 2017, **53**, 12140.

79. G. Fu, X. Yan, Y. Chen, L. Xu, D. Sun, J.-M. Lee and Y. Tang, *Adv. Mater.*, 2018, **30**, 1704609.

80. E. Hu, X. Y. Yu, F. Chen, Y. Wu, Y. Hu and X. W. Lou, *Adv. Energy Mater.*, 2018, **8**, 1702476.

81. T. Liu, F. Yang, G. Cheng and W. Luo, *Small*, 2018, **14**, 1703748.

82. P. Liu, D. Gao, W. Xiao, L. Ma, K. Sun, P. Xi, D. Xue and J. Wang, *Adv. Funct. Mater.*, 2018, **28**, 1706928.

83. S. Zhu, H. Tian, N. Wang, B. Chen, Y. Mai and X. Feng, *Small*, 2018, **14**, 1702755.